Am J Physiol Heart Circ Physiol 287: H994–H1002, 2004.
First published May 6, 2004; 10.1152/ajpheart.00400.2003.

Effect of shear stress on microvessel network formation of endothelial cells with in vitro three-dimensional model

Akinori Ueda,[1] Masaki Koga,[2] Mariko Ikeda,[3] Susumu Kudo,[4] and Kazuo Tanishita[2]

[1]*School of Fundamental Science and Technology,* [2]*Department of System Design Engineering, and* [3]*Keio Leading-Edge Laboratory of Science and Technology, Keio University, Yokohama 223-8522; and* [4]*Department of Mechanical Engineering, Shibaura Institute of Technology, Tokyo 108-8548, Japan*

Submitted 2 May 2003; accepted in final form 29 April 2004

Ueda, Akinori, Masaki Koga, Mariko Ikeda, Susumu Kudo, and Kazuo Tanishita. Effect of shear stress on microvessel network formation of endothelial cells with in vitro three-dimensional model. *Am J Physiol Heart Circ Physiol* 287: H994–H1002, 2004. First published May 6, 2004; 10.1152/ajpheart.00400.2003.—Shear stress stimulus is expected to enhance angiogenesis, the formation of microvessels. We determined the effect of shear stress stimulus on three-dimensional microvessel formation in vitro. Bovine pulmonary microvascular endothelial cells were seeded onto collagen gels with basic fibroblast growth factor to make a microvessel formation model. We observed this model in detail using phase-contrast microscopy, confocal laser scanning microscopy, and electron microscopy. The results show that cells invaded the collagen gel and reconstructed the tubular structures, containing a clearly defined lumen consisting of multiple cells. The model was placed in a parallel-plate flow chamber. A laminar shear stress of 0.3 Pa was applied to the surfaces of the cells for 48 h. Promotion of microvessel network formation was detectable after ~10 h in the flow chamber. After 48 h, the length of networks exposed to shear stress was 6.17 (±0.59) times longer than at the initial state, whereas the length of networks not exposed to shear stress was only 3.30 (±0.41) times longer. The number of bifurcations and endpoints increased for networks exposed to shear stress, whereas the number of bifurcations alone increased for networks not exposed to shear stress. These results demonstrate that shear stress applied to the surfaces of endothelial cells on collagen gel promotes the growth of microvessel network formation in the gel and expands the network because of repeated bifurcation and elongation.

angiogenesis; blood flow; capillary; in vitro model; migration

ANGIOGENESIS IS THE FORMATION of new microvessels (capillaries) by endothelial cells (ECs) migrating and proliferating from the preexisting vessel. This process is essential for numerous physiological events such as embryonic development, ovulation, and wound healing (14). Angiogenesis is also beneficial for tissue recovery by reperfusion of ischemic tissue but is maladaptive for arteriosclerosis, diabetes, and tumor growth (5).

Angiogenesis consists of a growth phase and a stabilization phase of microvessel formation (37). The growth phase involves four steps: *1*) dissolution of the basement membrane of the existing vessel and its surrounding extracellular matrix, *2*) migration and proliferation of ECs in the created space, *3*) lumen formation within the endothelial sprout, and *4*) formation of loops by anastomoses of sprouts. The stabilization phase involves three steps: *1*) arrest of EC proliferation, *2*) reconstruction of a basement membrane around the neovessels, and *3*) coverage of the immature capillary with pericytes.

Tumor development has a definite need for angiogenesis, and several angiogenic molecules have been identified, including fibroblast growth factor (FGF) and vascular endothelial growth factor (VEGF) families (9). In particular, basic FGF (bFGF) is necessary for vascular remodeling, and this cytokine is critical for new vessel formation (25, 39).

With three-dimensional (3-D) models, in vitro experiments have significantly advanced the understanding of angiogenesis. These models are based on the ability of stimulated ECs to invade substrates in a 3-D manner. When confluent cells cultured on gels are activated by cytokines such as bFGF (25) and VEGF (28) or by phorbol esters (24), they invade the underlying gel and form capillary-like structures. Compared with two-dimensional (2-D) models (e.g., Matrigel model), 3-D models more accurately represent an in vivo environment. In 3-D models, depending on the culture media composition, ECs are induced to sprout, proliferate, migrate, or differentiate in a 3-D manner (37).

Function and morphology of vascular systems are regulated by hemodynamic stress (31). Numerous studies report that wall shear stress affects vascular remodeling. For example, Kamiya and Togawa (18) reported that wall shear stress due to blood flow induces adaptive changes in blood vessel lumen in vivo. They suggested that the vessel is regulated to maintain a constant wall shear stress at its physiological level. Many in vitro studies using cultured ECs reported that application of fluid shear stress affects various cell functions and morphology (2, 8, 12, 34). Thus wall shear stress is a major factor influencing the adaptive vessel regulation for physiological as well as pathophysiological processes.

Shear stress also plays a role as a significant stimulus for angiogenesis. In vivo studies by Ichioka et al. (16) indicate that wound-healing angiogenesis is enhanced by the adaptive response of microvasculature to shear stress, and Nasu et al. (26) show that increased blood flow causes tumor vascular enlargement. Recent in vitro experiments by Gloe et al. (15) identify that shear stress induces capillary-like structure formation, and Cullen et al. (7) found that shear stress is a physiologically relevant stimulus for EC migration and angiogenesis.

However, in vivo studies on vascular remodeling need experimental manipulations such as atrioventricular shunt and vasodilator administration to alter hemodynamic conditions. The two in vitro studies by Gloe et al. (15) and Cullen et al. (7)

Address for reprint requests and other correspondence: A. Ueda, Tanishita Laboratory, Keio Univ., 3-14-1 Hiyoshi, Kohoku-ku, Yokohama 223-8522, Japan (E-mail: akinori@tani.sd.keio.ac.jp).

The costs of publication of this article were defrayed in part by the payment of page charges. The article must therefore be hereby marked "*advertisement*" in accordance with 18 U.S.C. Section 1734 solely to indicate this fact.

deal with capillary-like networks in 2-D models and primarily regard the networks as an evaluative criterion for physical and chemical stimulus. To clarify the details of the physiological and pathophysiological processes of angiogenesis under shear stress stimulus, 3-D networks of capillary-like structure must be reconstructed. We successfully reconstructed the 3-D network formation under shear stress stimulus. To assess the effect of shear stress on microvessel formation, we used an in vitro 3-D model in which ECs were induced by bFGF to invade a collagen gel. Bovine pulmonary microvascular ECs (BPMECs) were seeded onto collagen gels with bFGF and then placed in a parallel-plate flow chamber. A laminar shear stress of 0.3 Pa was applied to the surfaces of the ECs for 48 h. The total length of the networks was measured and used as an index of network formation. The density and the number of bifurcations and end points of the networks were measured to evaluate the morphology of the network. The migration velocity and direction of the ECs on the surface of collagen gel were measured to evaluate the influence of shear stress on the cells of the confluent monolayer of the 3-D model. We considered the effect that shear stress applied to the ECs on the surface of collagen gel had on the network formation in the gel. Our results reveal that shear stress induces network formation, enhances EC migration velocity, and affects both the direction of EC migration and the morphology of the network.

MATERIALS AND METHODS

Cell Culture

Cultured BPMECs were purchased from Cell Systems (lot no. 32030) and were used in all experiments. BPMECs had been used for in vitro experiments (13, 35) as capillary ECs; the property and culture methods of these cells have been established. These cells were cultured in Dulbecco's modified Eagle's medium (DMEM; no. 31600-34, GIBCO) supplemented with 10% fetal bovine serum (FBS; lot no. 9K2087, JRH Biosciences), 1% antibiotic-antimycotic (no. 15240-062, GIBCO), and 15 mM HEPES (no. 346-D1373, Dojinco). The BPMECs were seeded in 60-mm culture dishes (no. 430166, Corning) and cultivated under standard conditions (37°C, 5% CO_2). BPMECs were passaged by use of trypsin-EDTA (no. 25300-054, GIBCO). In our experiments, we used BPMECs passaged between five and nine times.

In Vitro Network Formation Assay

Collagen gels were prepared as follows: 8 vol of type I collagen solution (3.0 mg/ml; Cellmatrix Type I-A, Nitta Gelatin) were mixed with 1 vol of 5× DMEM and 1 vol of 0.1 N NaOH (no. 192-02175, Wako Pure Chemicals) on ice. The mixture was then poured into a glass-base dish (no. 3911-035, Iwaki) and allowed to gel at 37°C for 30 min.

BPMECs were seeded onto 1.53-mm-thick collagen gels at 4×10^5 cells per 35-mm culture dish. The cells reached confluence 72 h after seeding, and 30 ng/ml bFGF (Recombinant Human Fibroblast Growth Factor-basic, no. 100-18B, Pepro Tech) was added to the culture medium to promote network formation (25, 28). The ECs were then incubated at 37°C in 5% CO_2. After the addition of bFGF, the ECs invaded the underlying gel and began forming the network. This 3-D network model was used in the experiments.

Application of Shear Stress

Collagen gels with 3-D networks were placed into a parallel-plate flow chamber made of polycarbonate (Fig. 1), and the ECs grown on these collagen gels were subjected to well-defined laminar fluid shear stress by the flow of culture medium (DMEM). Flow of DMEM was provided by a sterile continuous-flow loop. Shear stress on ECs (τ, in Pa) was calculated by using the following formula

$$\tau = 6Q\mu/bh^2$$

where μ is fluid viscosity (8.5×10^{-4} Pa·s at 37°C), Q is flow rate (cm^3/s), h is the flow chamber height (0.2 mm), and b is the flow chamber width (20 mm). Because the main objective of this study was to show that the ability of microvasculature ECs to form new microvessel was modified under conditions of shear stress, the τ in the chamber was 0.30 ± 0.06 Pa for comparison with a previous in vivo study (16). The BPMECs were subjected to this τ for 48 h. The flowing culture medium was kept at 37°C in a water bath and was gassed with 5% CO_2-95% air to maintain pH 7.5 throughout the experiment. Bubbles were removed by a bubble trap. The perfusate was circulated by a roller pump (model MP-3N, Eyela) in the flow circuit. The total priming volume was 60 ml for the entire circuit. For control, the 3-D models were left at rest (static conditions, $\tau = 0$) under standard conditions (37°C, 5% CO_2) throughout the experiments.

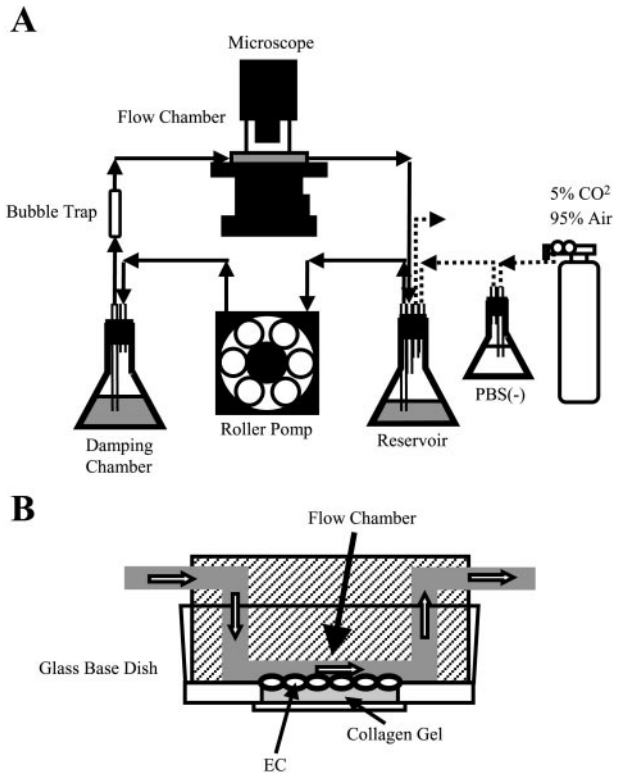

Fig. 1. Apparatus to apply shear stress to endothelial cells (ECs). *A*: flow chamber (dark shading) placed on the stage of a phase-contrast microscope was connected to a continuous flow circuit of culture medium (DMEM; arrows) and gas (5% CO_2-95% air; dashed line). *B*: ECs (ovals) on collagen gel (light shading) were subjected to shear stress by flow of DMEM (open arrows) for 48 h. Height and width of the flow chamber were 0.2 and 20 mm, respectively.

Images of the Growth of 3-D Networks

To observe the 3-D networks, ECs were photographed using a phase-contrast microscope (Eclipse TE300, Nikon) equipped with a CCD camera (CoolSNAP HQ, Roper Scientific). Phase-contrast images of the networks formed in collagen gels were recorded at 10-min intervals for 48 h with a microscope equipped with a time-lapse system (MetaMorph-HDTL, Roper Scientific).

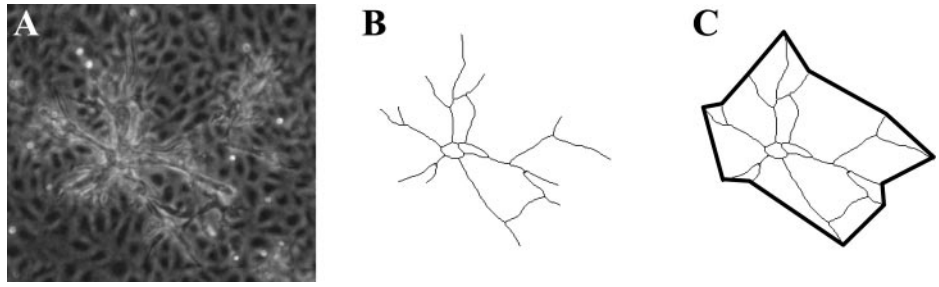

Fig. 2. Measurements of the network length, density, and centroid. *A*: phase-contrast image of network formation model under static conditions. *B*: how the total length of the network was quantified from the phase-contrast image. *C*: how the area connecting the end points was quantified.

Images of the Structure of 3-D Networks

The 3-D network models under static conditions were dyed with CellTracker Green BODIPY (no. C-2102, Molecular Probes) to observe the 3-D structure of the network in detail. After 3-D networks were formed, the collagen gel sample was washed in serum-free culture medium. CellTracker at 25 mM concentration was added, and the network was incubated for 45 min at 37°C. After the sample was washed in serum-free culture medium, the images were recorded by using a laser scanning confocal microscope (model no. MRC-600, Bio-Rad) with a ×20 objective lens. The emission of BODIPY excited at a wavelength of 488 nm with 25-mW argon ion lasers was detected in the wavelength region longer than 515 nm. Images were recorded every 5 μm in depth, starting from the confluent layer.

Images of the Altitudinal Structure of the 3-D Networks

The structure of 3-D network models under static conditions was observed based on images obtained by using electron microscopy. The samples were prepared for electron microscopy as follows. The static-conditioned 3-D network model was fixed overnight with 2.5% glutaraldehyde in 0.1 M sodium cacodylate buffer (pH 7.4) (no. S-009, TAAB). The cells were washed in 0.1 M sodium cacodylate buffer, postfixed in 1% osmium tetroxide in veronal acetate buffer for 2 h, dehydrated in 70–100% ethanol for 30 min, and finally embedded in epon. Semithin sections (1 μm) and thin sections (800–1000 Å) were sliced perpendicular to the culture plane by using an LKB ultramicrotome. The thin sections were stained with uranyl acetate and lead citrate. The images were obtained by using an electron microscope (model JEM-100S, JEOL).

Measurement of Network Morphology and EC Migration Using 2-D Parameters

Although there were 3-D networks in the gel, we used 2-D parameters because the formation of networks in a horizontal direction to the collagen surface was much larger than that in a perpendicular direction. The acquired phase images were analyzed by using a scion image analyzer (Scion). When we measured the following parameters, we focused only on 1 network/dish. As ECs began forming the network all over the dish 24 h after the addition of bFGF, there were >500 early networks in the dish, and 1 network near the center of the culture dish was randomly selected for analysis. The growth of the network was quantified by determining the total additive length of the network (Fig. 2, *A* and *B*). The network density was calculated from the total additive length of the network divided by the area enclosing all the endpoints of the network (Fig. 2*C*). The network length and its density with time were respectively normalized by the initial length and density (i.e., at 0 h of applied shear stress). Coordinates of the network centroid were calculated as follows:

$$x = \Sigma x_i / n$$

$$y = \Sigma y_i / n$$

where x_i and y_i are the *x*- and *y*-coordinates, respectively, of the *i*th point along the network (Fig. 2*B*) and *n* is the total additive number of coordinates in each image.

Migration velocity and direction of ECs on the surface of collagen gel were calculated by tracking a single cell in the phase-contrast images. Because these images were recorded at 10-min intervals for 48 h, it was easy to detect the successive movements of individual cells. We randomly chose some cells in the region near the network centroid (the distance in the direction parallel to collagen surface between the network centroid and the cell was within 100 μm) and some cells far from the centroid (over 100 μm) and tracked each cell. The downstream direction of the flow was defined as 0°.

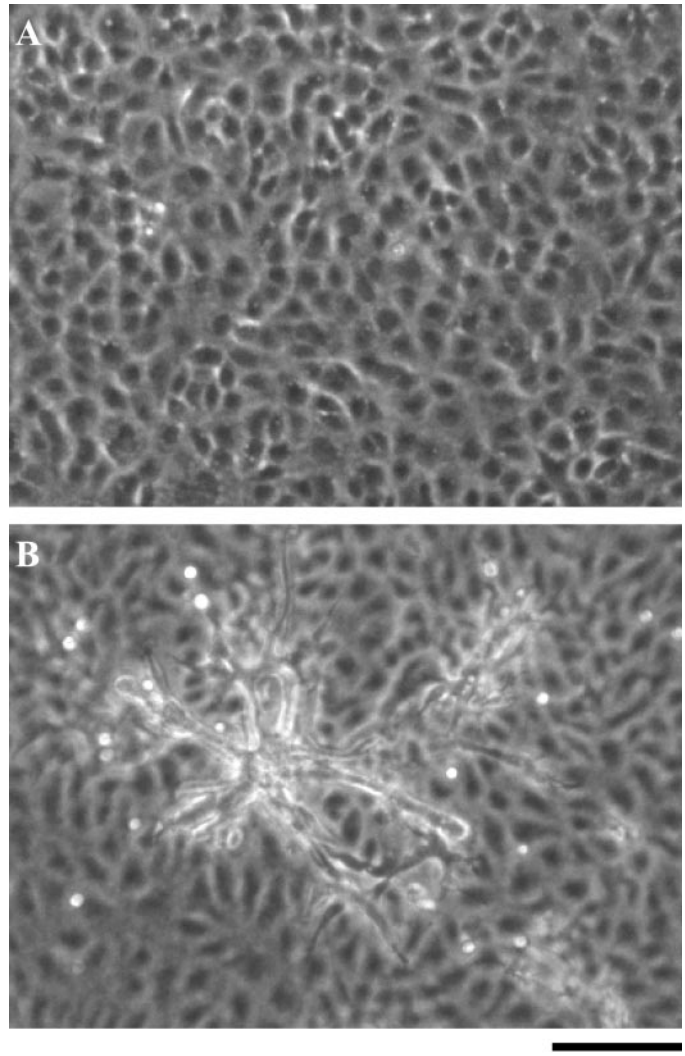

Fig. 3. In vitro model of three-dimensional (3-D) network formation. ECs were grown to confluence on the surface of collagen gel (*A*) and incubated with basic fibroblast growth factor (bFGF; 30 ng/ml; *B*) for 48 h under static conditions. Bar scale, 100 μm.

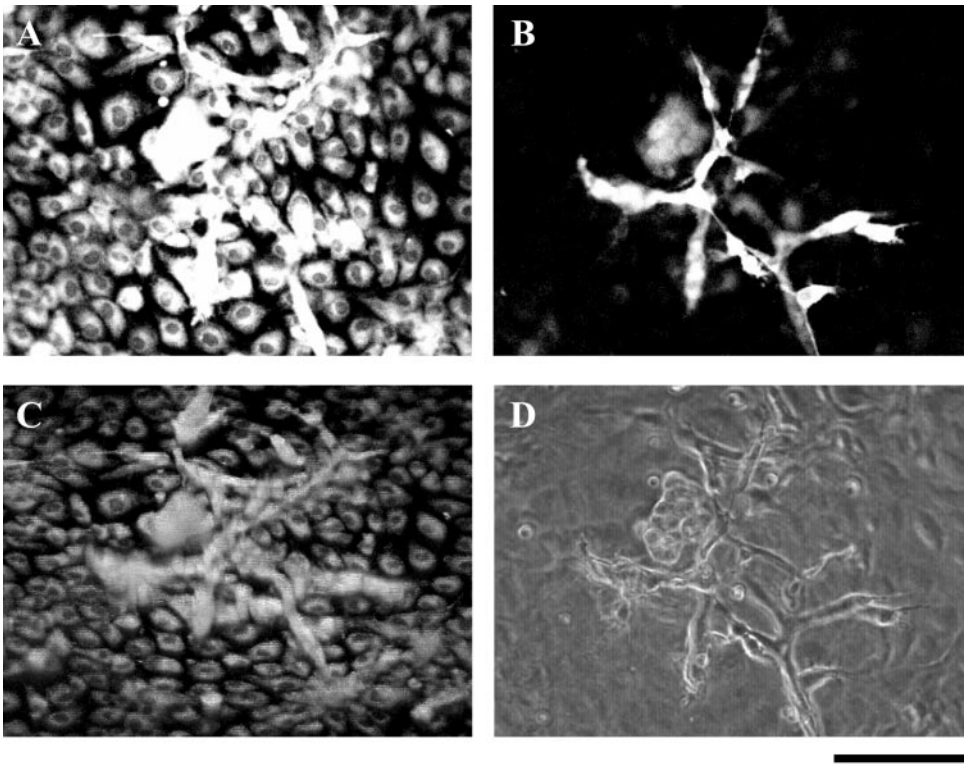

Fig. 4. Fluorescent image of 3-D network formation model under static conditions. *A* and *B*: fluorescent image of confluent monolayer (*A*) and structure 20 μm below the confluent monolayer (*B*). *C* and *D*: fluorescent image (*C*) and phase-contrast image (*D*) of the 3-D structure of the network. Bar scale, 100 μm.

Statistical Analysis

Data are presented as means ± SD. The number of replicated experiments performed is *n*. Student's *t*-test was used to test for differences, which were considered significant at an error level of $P < 0.05$. With the use of the *F*-test, the equality of variances of the direction of EC migration on the gel was tested for all pairs of variables.

RESULTS

Structure of the 3-D Network Formation Model

Growth factor bFGF enhanced the network formation in vitro. To assess the effect of shear stress on microvessel formation, we used an in vitro 3-D model in which ECs were induced to invade a collagen gel. BPMECs formed a confluent monolayer on the surface of the collagen gel 72 h after seeding (Fig. 3*A*), to which we added 30 ng/ml bFGF. Twenty-four hours after the addition of bFGF, the cells had invaded the underlying gel to begin forming the networks, which was slightly beneath the original monolayer. After 48 h of incubation with bFGF, these cells organized into branching capillaries and formed an extensive network under the surface monolayer (Fig. 3*B*), as in previous studies (25, 28).

3-D network model reached a depth of 50 μm. To observe the 3-D structure of the network in detail, the ECs were dyed with CellTracker after 72 h of incubation with bFGF, and images were recorded every 5 μm in depth, starting from the confluent layer by using confocal laser scanning microscopy. These images were used to clarify the 3-D structure of the network with the help of image analysis software. The results clearly show that cells invaded the collagen gel (Fig. 4) and reached a depth of up to 50 μm.

Images of thin sections perpendicular to the collagen surface obtained by use of electron microscopy confirmed that the ECs reconstructed the tubular structures, containing a clearly defined lumen consisting of multiple cells (Fig. 5).

Effect of Shear Stress on Microvessel Network Formation

Shear stress enhanced the growth of the microvessel network. To investigate the effect of shear stress on network formation, cells were incubated with bFGF for 24 h and then

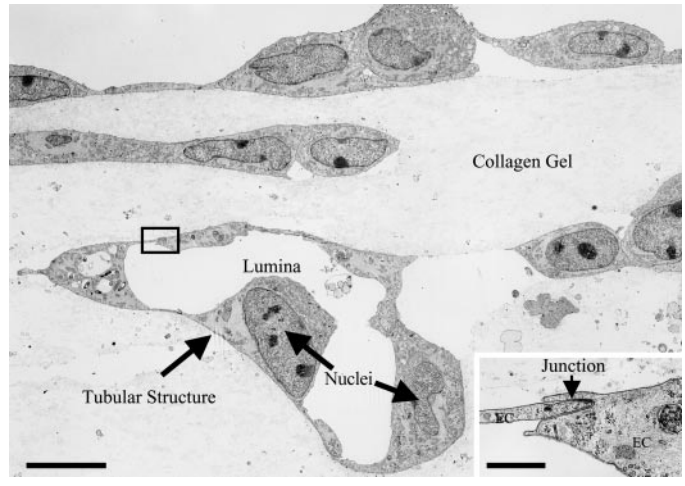

Fig. 5. Structure of 3-D network formation model under static conditions. Thin sections perpendicular to the culture plane of endothelial cells incubated with bFGF. Tubular structures composed of some cells enclosing lumina have formed inside the collagen gel. Bar scale, 10 μm. *Inset*: close-up view of outlined area, showing the junction between 2 ECs. Bar scale, 1 μm.

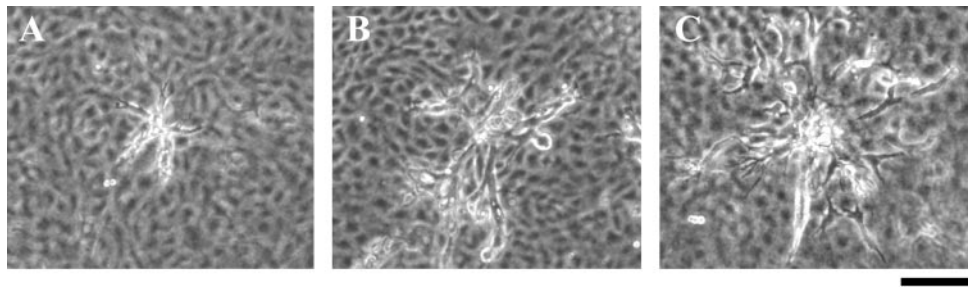

Fig. 6. Typical networks under shear stress and static conditions. *A*: network at the start of experiment (0 h). *B* and *C*: network at the end of experiment (48 h). *B*: network under static condition. *C*: network under shear-loaded condition. The direction of flow is *left* to *right*. The network under shear-loaded condition expanded wider than that under static condition. Bar scale, 100 μm.

subjected to laminar shear stress or left at static condition for 48 h (Fig. 6). The total length of the network was measured as an index of network formation. Results show that after 9 h (Fig. 7), applied shear stress did not significantly affect the network formation; the total length of the network under applied shear stress increased by a factor of 1.38 ± 0.14 compared with the initial length (i.e., at 0 h of applied shear stress), similar to the increase under static conditions (1.42 ± 0.13). After ~10 h, however, applied shear stress started to enhance the network formation (Fig. 7) compared with network formation under static conditions. After 24 h, the enhancement was significant; the network length increased by a factor of 3.13 ± 0.46 under applied shear stress compared with 2.17 ± 0.29 for static conditions ($P < 0.01$). After 48 h, the enhancement reached a maximum: a factor of 6.17 ± 0.59 under applied shear stress, compared with 3.30 ± 0.41 for static conditions ($P < 0.01$), indicating that the total length under applied shear stress was 1.87 times longer than under static conditions. These results clearly show that the 3-D network formation was significantly enhanced by shear stress loading.

Effect of shear stress on network density and number of bifurcations and end points. The network density gradually decreased with time and was independent of applied shear stress (Fig. 8).

The number of bifurcations and endpoints of a network are important geometrical parameters to evaluate the network growth process. The number of bifurcations of the networks increased with time, under either shear stress or static conditions, and there was no statistically significant difference (Fig. 9*A*). The number of end points increased at a similar rate under both shear stress and static conditions until ~10 h, after which the number under shear stress conditions increased further, whereas those under static conditions did not. The maximum increase in the number of end points under shear stress conditions (at 42–45 h) was >4 times higher than that under static conditions (Fig. 9*B*).

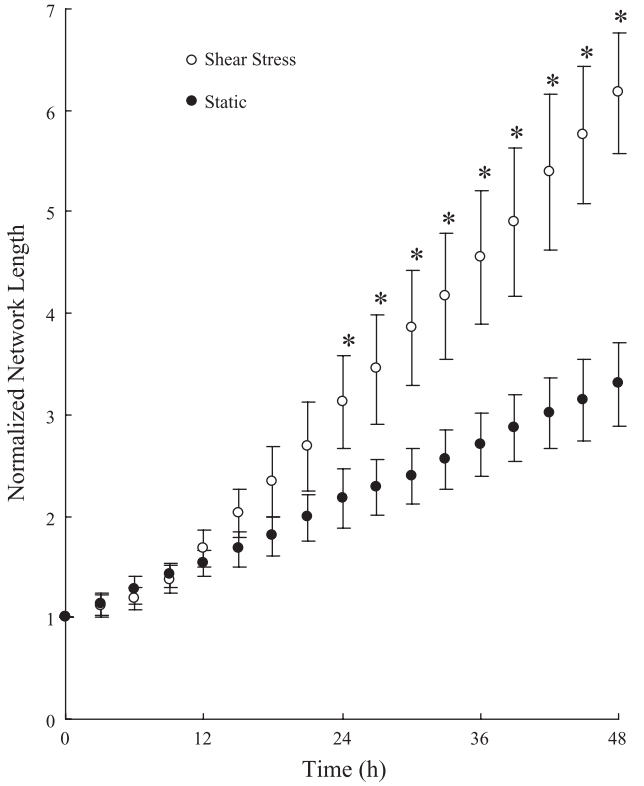

Fig. 7. Effect of shear stress on network length. Total length of the network under shear stress and static conditions was calculated every 3 h. Total length was normalized by the initial total length (i.e., at 0 h). Data are means ± SD; $n = 6$. *$P < 0.01$ vs. static cultures.

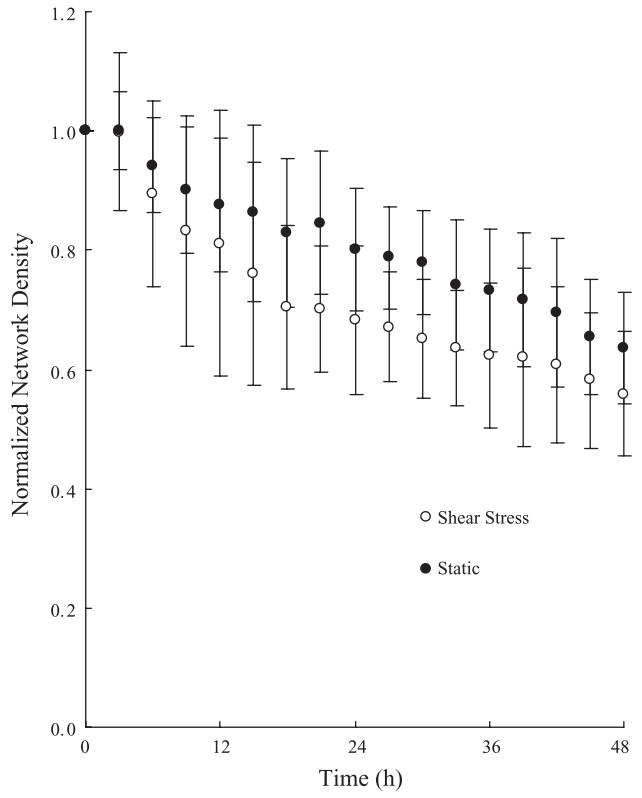

Fig. 8. Effect of shear stress on network density. Density of the network under shear stress and static conditions was calculated every 3 h. Density was normalized by the initial density (i.e., at 0 h). Data are means ± SD; $n = 6$.

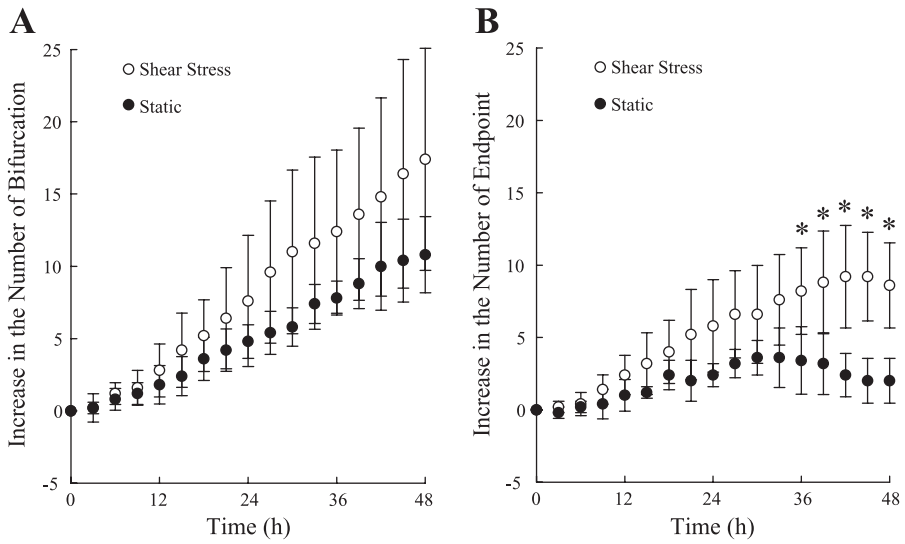

Fig. 9. Effect of shear stress on bifurcations (*A*) and endpoints of networks (*B*). Bifurcations and end points of network under shear stress and static conditions were calculated for every 3 h. Data are means ± SD; $n = 5$. *$P < 0.05$ vs. static cultures.

Effect of Shear Stress on the ECs of the Surface of Collagen Gel

Increase in migration velocity due to shear stress and bFGF. To estimate the influence of shear stress on the cells of the surface of the gel of this 3-D network formation model, we measured the migration velocity of the cells every hour up to 24 h (Fig. 10). The migration velocity of cells under applied shear stress (24 h, 9.46 ± 4.29 μm/h; $n = 64$) was significantly higher than that of cells under static conditions (6.40 ± 4.03 μm/h; $n = 77$, $P < 0.01$). Similarly, the migration velocity of cells treated with bFGF (24 h, 6.40 ± 4.03 μm/h; $n = 77$) was significantly higher than that of cells without bFGF (4.03 ± 2.48 μm/h; $n = 29$, $P < 0.01$).

Effect of shear stress-induced EC migration velocity on network formation. To evaluate the effect of EC migration of the surface of the gel on the network formation, we measured the migration velocity at 20–24 h (as a representative time) as a function of distance from the network centroid (Fig. 11). Under shear stress conditions, the migration velocity was lower near to the network centroid (<100 μm). By contrast, under static conditions, the migration velocity was relatively constant throughout the network.

Effect of shear stress on the migration direction of ECs. To determine the effect of shear stress on the migration direction of ECs on the surface of the gel, we measured the angle of EC migration at 20–24 h (as a representative time). The downstream direction of the flow was defined as 0°. The direction of shear-induced EC migration (Fig. 12*A*) was ~0° in the region far from the network centroid (>100 μm) but was random near the network centroid (<100 μm). Using the *F*-test, we showed

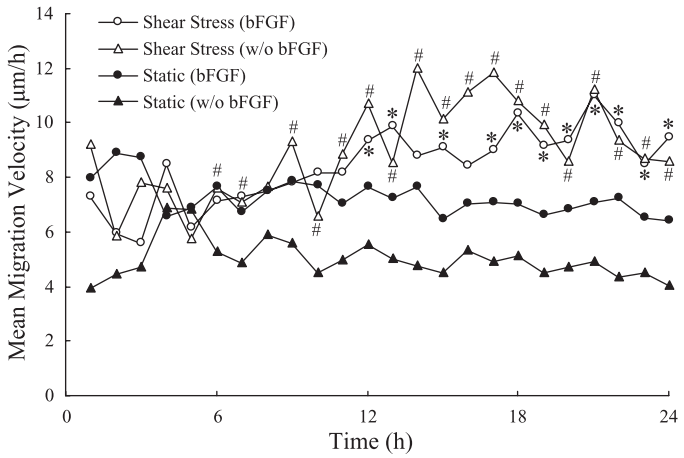

Fig. 10. Effect of shear stress and growth factor on migration velocity of ECs on the surface of collagen gel. Mean velocity of migration of ECs under shear stress and static conditions was calculated for each hour. Data are means; $n = 64$, flow (bFGF); 25, flow [without (w/o) bFGF]; 77, static (bFGF); and 29, static (w/o bFGF). *$P < 0.05$, flow (bFGF) vs. static (bFGF); #$P < 0.05$, flow (w/o bFGF) vs. static (w/o bFGF).

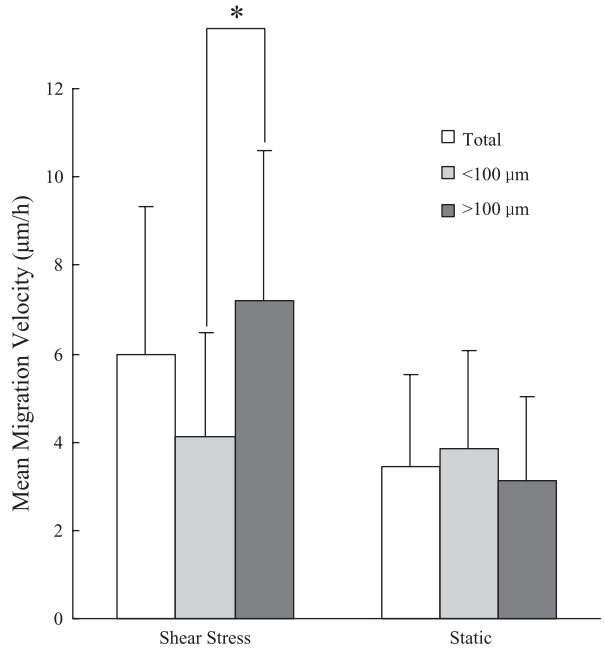

Fig. 11. Effect of shear stress on migration velocity of ECs on the surface of collagen gel. ECs, some of which were near the network (<100 μm) and some far from it (>100 μm), were tracked. Migration velocity of ECs under shear stress and static conditions was calculated at 20–24 h (as a representative of time) of applied shear stress and static culture. Data are means ± SD; $n = 80–90$. *$P < 0.01$.

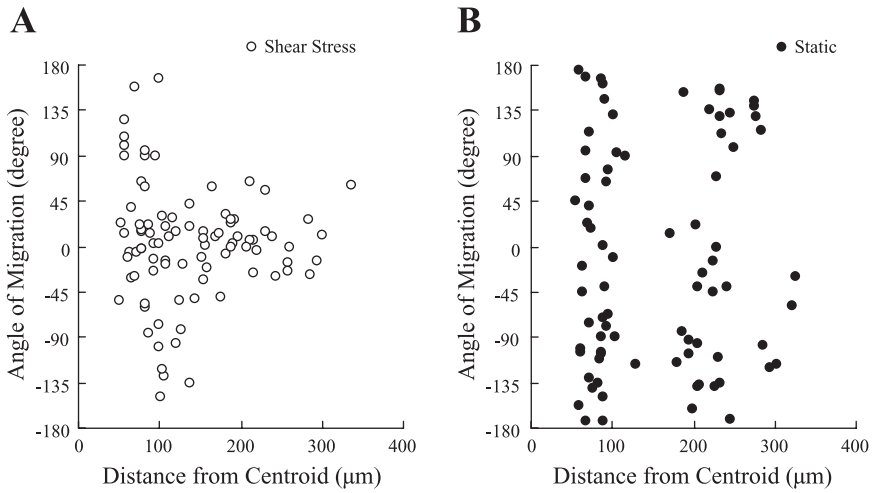

Fig. 12. Effect of shear stress on migration direction of ECs on the surface of collagen gel. ECs, some of which were near the network (<100 μm) and some far from it (>100 μm), were tracked. Angle of EC migration at 20–24 h (as a representative of time) of applied shear stress (*A*) and that under static condition (*B*). Downstream direction of the flow was defined as 0°; n = 80–90. *A*: direction of shear-induced EC migration was ~0° in the region far from the network centroid, whereas the direction was random near the network centroid. The variances in the direction of EC migration display a significant difference (F-test, $P < 0.05$) between the region near the centroid and that far from the network centroid. *B*: under static conditions, the migration direction of ECs was random all over the place, and there is no significant difference in the variances of the migration direction.

that the variances in the direction of EC migration display a significant difference ($P < 0.05$) between the region far from the network centroid and the region near the network centroid. In contrast, the direction of cells under static conditions was random throughout the network (Fig. 12*B*), and there is no significant difference in the variances of the migration direction.

DISCUSSION

Structure of the 3-D Network Formation Model

At a bFGF concentration of 30 ng/ml in the culture medium, 3-D formation of a capillary-like structure by ECs in the collagen gel was successfully reconstructed. The presence of bFGF is essential for network formation (25, 28). bFGF induces production of interstitial collagenase in the cultured ECs and augments the formation process of new capillaries (32). In our model, the bFGF then induced new capillary-like structures to invade the underlying collagen gel (Fig. 3), and the newly formed structures organized themselves as distinct tubules resembling blood capillaries (Fig. 5).

ECs in the collagen gel constructed a lumen (Fig. 5). The lumen of the network consisted of a few cells, together with a gap junction. Most networks reached a depth of ~20 μm, with a maximum depth of ~50 μm from the root of the network to the tip. By using three different types of microscopy (phase contrast, confocal laser scanning, and electron) and a dye (CellTracker), we revealed the network formation process, including the destruction of capillary basement membranes, migration, and formation into capillary structures.

Effect of Shear Stress on 3-D Network Formation

A correlation between blood flow and angiogenesis in vivo has been reported (16, 26). For example, Ichioka et al. (16) showed that the blood flow in vessels influenced angiogenesis. They used vasodilator prazosin to modify the blood flow and found that angiogenesis during wound healing in the rabbit ear chamber was positively influenced by elevated prazosin-induced shear stress. Nasu et al. (26) observed growing tumor vessels in vivo to elucidate the relationship between blood flow and vascular enlargement and showed that tumor angiogenesis depended more on local hemodynamics than on vascular growth factors. In an in vitro study, Albuquerque et al. (1) demonstrated that physiological shear stress enhances wound closure in cultured human umbilical vein and coronary artery ECs through the action of EC spreading and migration. In another in vitro study, Urbich et al. (36) indicated that the shear stress-induced migration was independent of cell proliferation but was dependent on the fibronectin receptor-$\alpha_5\beta_1$. Only a few studies, however, have quantified the relationship between network formation and shear stress. Recent in vitro studies showed that flow induced the growth of the network formation of ECs in a 2-D model (7, 15). In our study, we successfully reconstructed a 3-D network formation model that mimics the conditions of an in vivo environment (37). The application of shear stress on the ECs resulted in an increased length of the entire network after ~10 h (Fig. 7), the same time that active migration of cells on the collagen gel began (Fig. 10).

This refractory period, which required transmitting the effect of shear stress to EC features, was thought to be similar to previous studies. Franke et al. (10) showed that the endothelial stress fibers could be induced by a 3-h exposure of shear stress of 0.2 Pa, and Ookawa et al. (27) indicated that a stress fiber-like structure was formed by a 3-h exposure of shear stress of 2.0 Pa. Wechezak et al. (38) exposed ECs to a shear stress of 0.93 Pa for 2 h and observed that microfilament bundles and their associated focal contacts were concentrated in the proximal cell regions. As just described, these changes in cytoskeleton and adherence protein need several hours and probably cause the refractory period of EC migration and network formation. For EC migration, Tanishita et al. (34) also observed ECs under shear stress of 5 Pa in which migration velocity was 1–5 μm/h initially and accelerated slightly after 12–16 h, finally reaching ~16 μm/h after 16 h. In our study, we observed that ECs required ~10 h to transmit the effect of shear stress to not only EC migration but also network formation. Our study also revealed that the migration velocity and direction of ECs on the confluent surface depended on the distance from the network centroid (Figs. 11 and 12). Thus the nature of cellular migration strongly affects the network formation in the gel.

Numerous previous studies focused on relationships between shear stress and growth factors such as bFGF and VEGF. For example, Gloe et al. (15) demonstrated that shear

stress induced the release of bFGF from ECs, and Malek et al. (22) reported that laminar shear stress induced bFGF mRNA expression. Milkiewicz et al. (23) reported that higher capillary shear stress increases VEGF expression, whereas Conklin et al. (6) reported that low shear stress increases VEGF expression in ECs. Furthermore, NO is associated with angiogenesis. For example, Smith et al. (33) reported that endothelial nitric oxide (NO) synthase enhances angiogenesis, and Lee et al. (20) showed that NO induces angiogenesis in vivo and in vitro by promoting EC migration and differentiation into capillaries. Lee et al. also demonstrated that NO increased $\alpha_v\beta_3$-integrin expression in ECs, a critical mediator of EC-matrix adhesion and migration. Although proteolysis is a key step in angiogenesis, matrix metalloproteinase does not increase after stimulation by shear stress (29). Our results show that in the presence of bFGF, the migration velocity of ECs without applied shear stress (static conditions) only slightly increased, whereas that of ECs under shear stress conditions significantly increased (Fig. 10).

Our results show that the network density was relatively unaffected by the shear stress (Fig. 8). To determine the effect of shear stress on the process of network formation, we measured the number of bifurcations and endpoints of the networks under shear stress and static conditions. Networks under static conditions showed slow elongation and bifurcation (Figs. 7 and 9*A*), resulting in the fusion of some tips, and thus the number of endpoints only slightly increased (Fig. 9*B*). In contrast, under shear stress conditions, the end points of network branches were often extended, and the networks widely expanded with progressive elongation and bifurcation (Fig. 7 and 9*A*), resulting in an increase in the number of bifurcations and end points (Fig. 9).

As observed above, this model reproduced well new microvessel formation in vivo, and we could study about the effect of shear stress on that. There were, however, some points which could not be reproduced in this model. Capillary networks in vivo may have different outcomes because the matrix in this model, pure type I collagen gel, is not the typical matrix found in vivo, and matrix composition may play important roles in angiogenesis modulation (17, 21). The fact that expression of integrin may also be different from an in vivo environment possibly affects tube formation and migration of ECs. As for $\alpha_v\beta_3$-integrin, it plays a critically important role in angiogenesis by bFGF in both an in vitro and an in vivo environment (4, 11, 19, 30). Furthermore, endothelial progenitor cells (EPCs) also participate in new vessel formation in vivo (3), but we did not focus on EPCs in this study. We believe nonetheless that this experimental setup, the combination of a 3-D network formation model and shear loading application, is beneficial in showing that the ability of microvasculature ECs to form new microvessels was modified under conditions of shear stress vs. no shear stress.

In summary, shear stress promoted the growth of 3-D network formation in vitro. The enhancement became detectable 10 h after the initiation of shear stress. After 48 h, the growth rate (i.e., increase in network length) of a network under shear stress conditions was approximately two times faster than that of a network under static conditions. Furthermore, shear stress applied to ECs on the surface of collagen gel influenced the process of network formation in the gel. The end points of the network branches were extended, and the networks were significantly expanded because of repeated bifurcation and elongation.

REFERENCES

1. **Albuquerque ML, Waters CM, Savla U, Schnaper HW, and Flozak AS.** Shear stress enhances human endothelial cell wound closure in vitro. *Am J Physiol Heart Circ Physiol* 279: H293–H302, 2000.
2. **Ando J, Tsuboi H, Korenaga R, Takada Y, Toyama-Sorimachi N, Miyasaka M, and Kamiya A.** Shear stress inhibits adhesion of cultured mouse endothelial cells to lymphocytes by downregulating VCAM-1 expression. *Am J Physiol Cell Physiol* 267: C679–C687, 1994.
3. **Asahara T, Murohara T, Sullivan A, Silver M, van der Zee R, Li T, Witzenbichler B, Schatteman G, and Isner JM.** Isolation of putative progenitor endothelial cells for angiogenesis. *Science* 275: 964–967, 1997.
4. **Brooks PC, Clark RA, and Cheresh DA.** Requirement of vascular integrin αvβ3 for angiogenesis. *Science* 264: 569–571, 1994.
5. **Carmeliet P and Jain RK.** Angiogenesis in cancer and other diseases. *Nature* 407: 249–257, 2000.
6. **Conklin BS, Zhong DS, Zhao W, Lin PH, and Chen C.** Shear stress regulates occludin and VEGF expression in porcine arterial endothelial cells. *J Surg Res* 102: 13–21, 2002.
7. **Cullen JP, Sayeed S, Sawai RS, Theodorakis NG, Cahill PA, Sitzmann JV, and Redmond EM.** Pulsatile flow-induced angiogenesis: role of Gi subunits. *Arterioscler Thromb Vasc Biol* 22: 1610–1616, 2002.
8. **Fisher AB, Chien S, Barakat AI, and Nerem RM.** Endothelial cellular response to altered shear stress. *Am J Physiol Lung Cell Mol Physiol* 281: L529–L533, 2001.
9. **Folkman J and Shing Y.** Angiogenesis. *J Biol Chem* 267: 10931–10934, 1992.
10. **Franke RP, Grafe M, Schnittler H, Seiffge D, Mittermayer C, and Drenckhahn D.** Induction of human vascular endothelial stress fibres by fluid shear stress. *Nature* 307: 648–649, 1984.
11. **Friedlander M, Brooks PC, Shaffer RW, Kincaid CM, Varner JA, and Cheresh DA.** Definition of two angiogenic pathways by distinct αv integrins. *Science* 270: 1500–1502, 1995.
12. **Fukushima S, Nagatsu A, Kaibara M, Oka K, and Tanishita K.** Measurement of surface topography of endothelial cell and wall shear stress distribution on the cell. *JSME Int J C-Mech Sy* 44: 972–981, 2001.
13. **Garcia JG, Liu F, Verin AD, Birukova A, Dechert MA, Gerthoffer WT, Bamberg JR, and English D.** Sphingosine 1-phosphate promotes endothelial cell barrier integrity by Edg-dependent cytoskeletal rearrangement. *J Clin Invest* 180: 689–701, 2001.
14. **Gerwins P, Skoldenberg E, and Claesson-Welsh L.** Function of fibroblast growth factors and vascular endothelial growth factors and their receptors in angiogenesis. *Crit Rev Oncol Hematol* 34: 185–194, 2000.
15. **Gloe T, Sohn HY, Meininger GA, and Pohl U.** Shear stress-induced release of basic fibroblast growth factor from endothelial cells is mediated by matrix interaction via integrin αvβ3. *J Biol Chem* 277: 23453–23458, 2002.
16. **Ichioka S, Shibata M, Kosaki K, Sato Y, Harii K, and Kamiya A.** Effects of shear stress on wound-healing angiogenesis in the rabbit ear chamber. *J Surg Res* 72: 29–35, 1997.
17. **Iivanainen E, Kahari VM, Heino J, and Elenius K.** Endothelial cell-matrix interactions. *Microsc Res Tech* 60: 13–22, 2003.
18. **Kamiya A and Togawa T.** Adaptive regulation of wall shear stress to flow change in the canine carotid artery. *Am J Physiol Heart Circ Physiol* 239: H14–H21, 1980.
19. **Kuzuya M, Satake S, Ramos MA, Kanda S, Koike T, Yoshino K, Ikeda S, and Iguchi A.** Induction of apoptotic cell death in vascular endothelial cells cultured in three-dimensional collagen lattice. *Exp Cell Res* 248: 498–508, 1999.
20. **Lee PC, Kibbe MR, Schuchert MJ, Stolz DB, Watkins SC, Griffith BP, Billiar TR, and Shears LL II.** Nitric oxide induces angiogenesis and upregulates avb3 integrin expression on endothelial cells. *Microvasc Res* 60: 269–280, 2000.
21. **Madri JA and Williams SK.** Capillary endothelial cell cultures: phenotypic modulation by matrix components. *J Cell Biol* 97: 153–165, 1983.
22. **Malek AM, Gibbons GH, Dzau VJ, and Izumo S.** Fluid shear stress differentially modulates expression of genes encoding basic fibroblast growth factor and platelet-derived growth factor B chain in vascular endothelium. *J Clin Invest* 92: 2013–2021, 1993.

23. **Milkiewicz M, Brown MD, Egginton S, Hudlicka O.** Association between shear stress, angiogenesis, and VEGF in skeletal muscles in vivo. *Microcirculation* 8: 229–241, 2001.
24. **Montesano R and Orci L.** Tumor-promoting phorbol esters induce angiogenesis in vitro. *Cell* 42: 469–477, 1985.
25. **Montesano R, Vassalli JD, Baird A, Guillemin R, and Orci L.** Basic fibroblast growth factor induces angiogenesis in vitro. *Proc Natl Acad Sci USA* 83: 7297–7301, 1986.
26. **Nasu R, Kimura H, Akagi K, Murata T, and Tanaka Y.** Blood flow influences vascular growth during tumour angiogenesis. *Br J Cancer* 79: 780–786, 1999.
27. **Ookawa K, Sato M, and Ohshima N.** Changes in the microstructure of cultured porcine aortic endothelial cells in the early stage after applying a fluid-imposed shear stress. *J Biomech* 25: 1321–1328, 1992.
28. **Pepper MS, Ferrara N, Orci L, and Montesano R.** Leukemia inhibitory factor (LIF) inhibits angiogenesis in vitro. *J Cell Sci* 108: 73–83, 1995.
29. **Rivilis I, Milkiewicz M, Boyd P, Goldstein J, Brown MD, Egginton S, Hansen FM, Hudlicka O, and Haas TL.** Differential involvement of MMP-2 and VEGF during muscle stretch- versus shear stress-induced angiogenesis. *Am J Physiol Heart Circ Physiol* 283: H1430–H1438, 2002.
30. **Satake S, Kuzuya M, Ramos MA, Kanda S, and Iguchi A.** Angiogenic stimuli are essential for survival of vascular endothelial cells in three-dimensional collagen lattice. *Biochem Biophys Res Commun* 244: 642–646, 1998.
31. **Skalak TC and Price RJ.** The role of mechanical stresses in microvascular remodeling. *Microcirculation* 3: 143–165, 1996.
32. **Slavin J.** Fibroblast growth factors: at the heart of angiogenesis. *Cell Biol Int* 19: 431–444, 1995.
33. **Smith RS Jr, Lin KF, Agata J, Chao L, and Chao J.** Human endothelial nitric oxide synthase gene delivery promotes angiogenesis in a rat model of hindlimb ischemia. *Arterioscler Thromb Vasc Biol* 22: 1279–1285, 2002.
34. **Tanishita K, Nagayama K, Fujii M, and Kudou S.** Empirical study on grouping behavior of individual endothelial cells under shear stress. *JSME Int J C-Mech Sy* 42: 715–720, 1999.
35. **Tomii Y, Kamochi J, Yamazaki H, Sawa N, Tokunaga T, Ohnishi Y, Kijima H, Ueyama Y, Tamaoki N, Nakamura M.** Human thrombospondin 2 inhibits proliferation of microvascular endothelial cells. *Int J Oncol* 20: 339–342, 2002.
36. **Urbich C, Dernbach E, Reissner A, Vasa M, Zeiher AM, and Dimmeler S.** Shear stress-induced endothelial cell migration involves integrin signaling via the fibronectin receptor subunits α5 and β1. *Arterioscler Thromb Vasc Biol* 22: 69–75, 2002.
37. **Vailhé B, Vittet D, and Feige JJ.** In vitro models of vasculogenesis and angiogenesis. *Lab Invest* 81: 439–452, 2001.
38. **Wechezak AR, Wight TN, Viggers RF, and Sauvage LR.** Endothelial adherence under shear stress is dependent upon microfilament reorganization. *J Cell Physiol* 139: 136–146, 1986.
39. **Yang HT, Ogilvie RW, and Terjung RL.** Exercise training enhances basic fibroblast growth factor-induced collateral blood flow. *Am J Physiol Heart Circ Physiol* 274: H2053–H2061, 1998.